Electronic Supplementary Material (ESI) for ChemComm.

Supporting Information

A Fluoride-Free Siliceous STW-Type Zeolite Synthesized Using a Designed Organic Structure-Directing Agent

Feng Jiao,[a] Jun Zhang,[b] Xianshu Cai,[a] Hao Li,[a] Yanan Xu,[a] Yue Zhao [a] and Hongbin Du*[a]

[a] State Key Laboratory of Coordination Chemistry School of Chemistry and Chemical Engineering, Nanjing University, Nanjing, 210023 (China)

[b] School of Materials and Chemistry Engineering Anhui Jianzhu University, Hefei, 230601 (China)

E-mail: hbdu@nju.edu.cn

Table of Contents

Experimental Procedures

Materials Preparation

Synthesis of OSDA(OH)

15 mL (0.1208 mol) of 1,5-diazabicyclo[4.3.0]non-5-ene and 15 mL (0.2409 mol) of methyl iodide were added into MeCN (150 mL). The mixture was heated at 45°C for 12 h. The product was obtained by filtration, purified by recrystallization with water to give a white solid after dried overnight at 80°C (30.73 g, yield: 96%). The iodine forms of the OSDA were converted into the hydroxides by anion exchange. The concentration of the OSDA(OH) was obtained by titration with HCl.

Synthesis of Si-STW-F

In a typical synthesis, 2 mmol of tetraethylorthosilicate (TEOS) were added into the solution of OSDA(OH) (1 mmol), and then the mixture was stirred until the complete hydrolysis of TEOS. 1 mmol of HF were dosed into the solution under stirring for 1 h. The gel was dried at 80°C to evaporate excess water and ethanol until the theoretical quantity was reached. The final gel with a composition of 1 SiO_2 : 0.5 OSDA(OH) : 0.5 HF. : 5 H_2O was transferred into a 15-mL-Teflon-lined stainless-steel autoclave and heated at 160°C for 15 d. The products (denoted as Si-STW-F) were collected by filtrating, washing and drying in air. The products were calcined at 550°C in air for 5 h to remove OSDAF.

Synthesis of Si-STW-OH

In a typical synthesis, 2 mmol of tetraethylorthosilicate were added into the solution of OSDA(OH) (1 mmol), and then the mixture was stirred until the complete hydrolysis of TEOS. In the cases of seeded syntheses, 0.005 g of zeolite seeds were then added. The gel was dried at 80°C to evaporate excess water and ethanol until the theoretical quality was reached. The final gel with a composition of 1 SiO_2 : 0.5 OSDA(OH) : 5 H_2O was transferred into a 15-mL-Teflon-lined stainless-steel autoclave and heated at 160°C for 40 d. The products (denoted as Si-STW-OH) were collected by centrifugation and drying in air. The products were calcined at 550°C in air for 5 h to remove OSDA(OH).

Characterizations

Powder X-ray diffraction (PXRD) patterns were performed on a Bruker D8 Advance instrument with a CuKα radiation (λ = 1.54056 Å) in the 2θ ranging from 5 to 50°. Scanning electron microscopy (SEM) images were collected on a field emission scanning electron microanalyzer (Hitachi S-4800). Thermogravimetric analyses (TGA) were carried out on a PerkinElmer thermal analyzer under a flowing air with a heating rate of 10 °C min^{-1}. Chemical analysis of C, H, and N was carried out on an Elementar Vario MICRO cube. N_2 gas adsorption was performed on the Micrometrics ASAP 2020 surface-area porosimetry system at 77 K. Liquid-state ^{13}C nuclear magnetic resonance (NMR) spectra were performed on a Bruker DRX-400 spectrometer. The ^{13}C MAS NMR spectra were acquired on a Bruker Avance 600 MHz spectrometer with a 100.62 MHz resonance frequency. The ^{29}Si MAS NMR spectra were recorded on a Bruker Avance 600 MHz spectrometer with a resonance frequency of 79.49 Hz and the $\pi/2$ pulse of 62.5 kHz. The ^{19}F MAS NMR spectra were recorded on a Bruker Avance 400 MHz spectrometer with a spinning rate of 14 kHz and pulse of 2.1 ms.

Single-crystal X-ray diffraction (SXRD) data was collected with a Bruker D8 Venture equipped with a Ga liquid-metal jet X-ray source (Excilum, Ga Kα 1.3414 Å). Data reduction and absorption corrections were performed by using the SAINT and SADABS programs,[1, 2] respectively. The structure was solved by using direct methods with the SHELEX-2018 program and refined with full-matrix least squares on F^2 by using the SHELEX-2018 program.[3] Deposition number 2211902 (for Si-STW-F) contains the supplementary crystallographic data for this paper. These data are provided free of charge by the joint Cambridge Crystallographic Data Centre and Fachinformationszentrum Karlsruhe Access Structures service.

Calculation methods

Theoretical calculations were performed to study the stabilization energies between the OSDAs and STW zeolite framework based on the DFT+D theory using the plane wave approaches implemented in CASTEP package.[4] The geometries of zeolites MDBN-Si-STW-F and ETMI-Si-STW-F [5] (space group $P6_1$) were taken from single crystal X-ray diffraction analyses. The $P6_1$ structure model for PMI-Si-STW-F was built manually in a similar manner by substitution of the OSDA cations from MDBN-Si-STW-F while the cell parameters were kept with the single crystal structure data of $P6_5$-symmetry PMI-Si-STW-F.[5] The geometry optimizations with fixed cell parameters were carried out with the generalized gradient approximation (GGA) method and the

Perdew-Burke-Ernzerhof (PBE)[6] as exchange-correlation functional. The dispersion correction scheme by Grimme (G06) was employed to account for the weak interactions.[7, 8] The periodic boundary conditions were employed to model the systems. The Brillouin zone was sampled by a *k*-point mesh of 1 × 1 × 1. An energy cutoff of 571.4 eV for the planewave basis set was used during the calculations. The self-consistent field (SCF) calculations were converged at 1×10^{-6} eV per atom. The convergence conditions for the optimization calculations were set with the energy change between two consecutive steps lower than 1×10^{-5} eV, and a maximum force allowed lower than 0.03 eV/Å on each atom. The interaction energy ($E_{interaction}$) of OSDA was defined as:

$$E_{interaction} = (E_{OSDAF@zeolite} - E_{zeolite} - nE_{OSDA} - nE_F)/nN_T \quad (1)$$

where $E_{OSDAF@zeolite}$ was the total energy of zeolite embedded with OSDAF, $E_{zeolite}$ was the energy of empty zeolite, E_{OSDA} was the energy of the OSDA cation, E_{OSDA} was the energy of the F^- anion, n is the number of OSDAF in zeolite, and N_T is the number of T sites in zeolite, respectively. In the unit cell of STW, n = 6 and N_T = 60.

Further studies on intermolecular interactions between the OSDAs and the zeolite framework were performed with softwares Multiwfn[9-11] and CP2K.[12, 13] The electron densities of the optimized OSDA-Si-STW-F were obtained with the GGA PBE method implemented in CP2K-2022.1 package using the molecularly optimized basis set DZVP-MOLOPT-SR-GTH and a Goedecker-Teter-Hutter (GTH) pseudopotential.[14-16] The dispersion correction scheme by Grimme (DFT-D3(BJ)) was employed to account for the weak interactions.[7, 8] An energy cutoff of 600 Ry and 60 Ry for the planewave and Gaussians mapping, respectively, was used during the calculations. The self-consistent field (SCF) calculations were converged at 1×10^{-6} Hartree. The electron density analyses such as electrostatic potential coloured van der Waals surface and independent gradient model on Hirshfeld partition of electron density were performed on Multiwfn and the results were visualized by VMD[17] and VESTA.[18]

Supplementary Figures

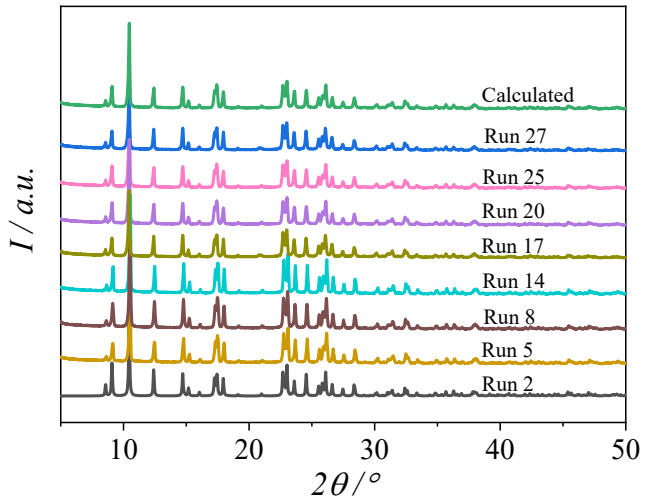

Figure S1. PXRD patterns of Si-STW-F synthesized under different synthesis conditions, compared to the calculated one based on the single crystal diffraction data of Si-STW-F.

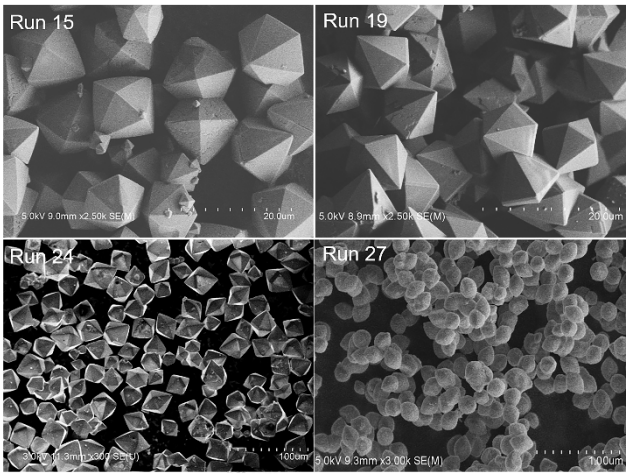

Figure S2. SEM images of Si-STW-F prepared under different synthesis conditions.

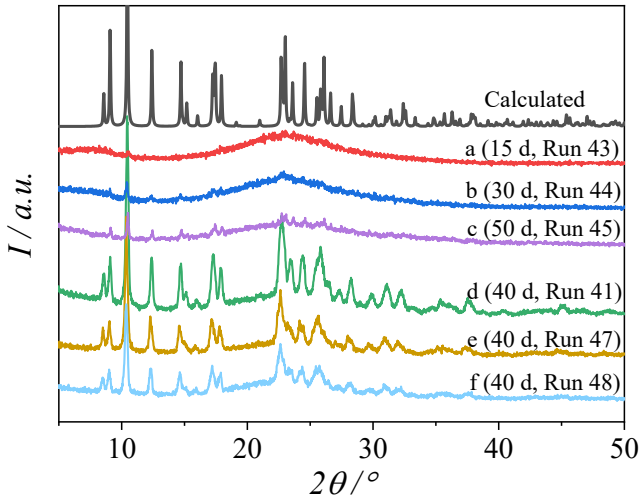

Figure S3. PXRD patterns of as-synthesized Si-STW-OH: (a, b, and c) without seeds, (d) with F-containing seeds, (e, f) with F-free seeds. The calculated one based on the single crystal diffraction data of Si-STW-F is shown for comparison.

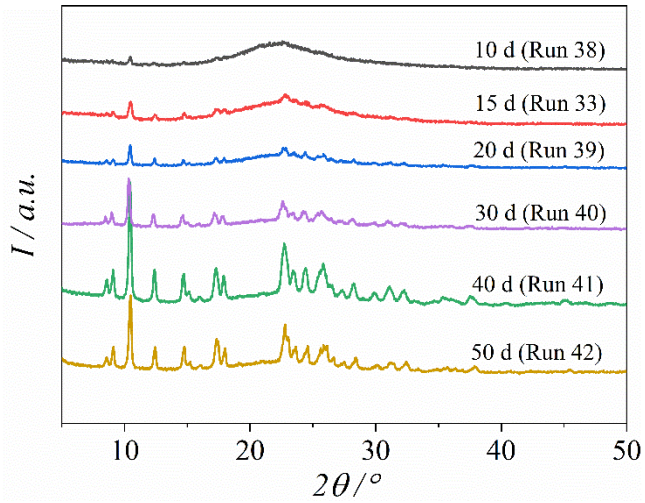

Figure S4. PXRD patterns of Si-STW-OH with seeded syntheses at different synthesis time. All peaks are assigned to STW.

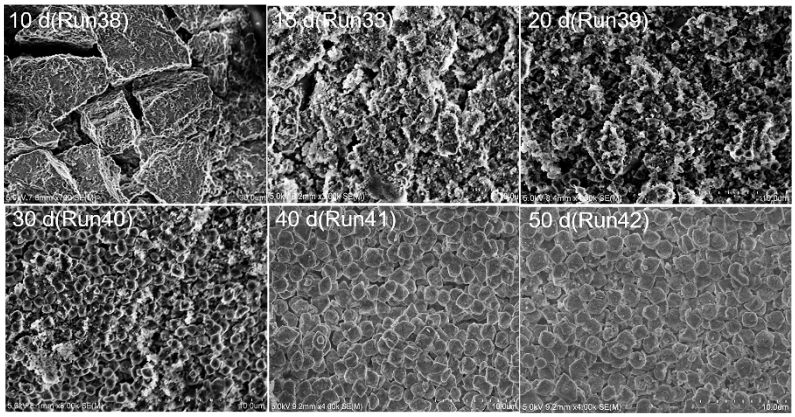

Figure S5. SEM images of Si-STW-OH synthesized with different synthesis time.

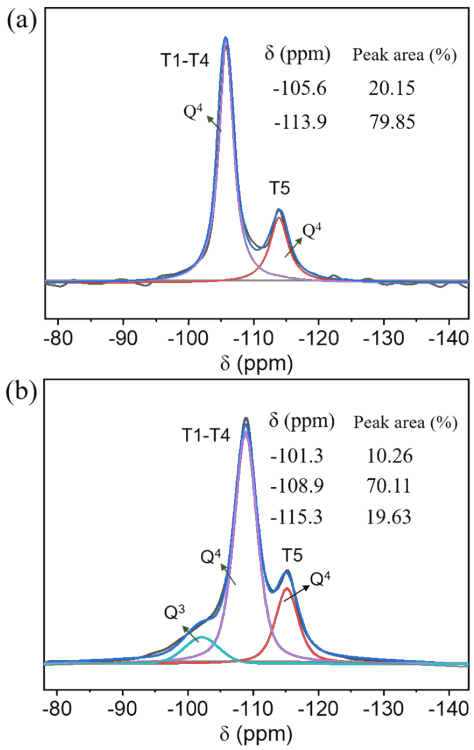

Figure S6. ^{29}Si MAS NMR spectra of as-made (a) Si-STW-F and (b) Si-STW-OH.

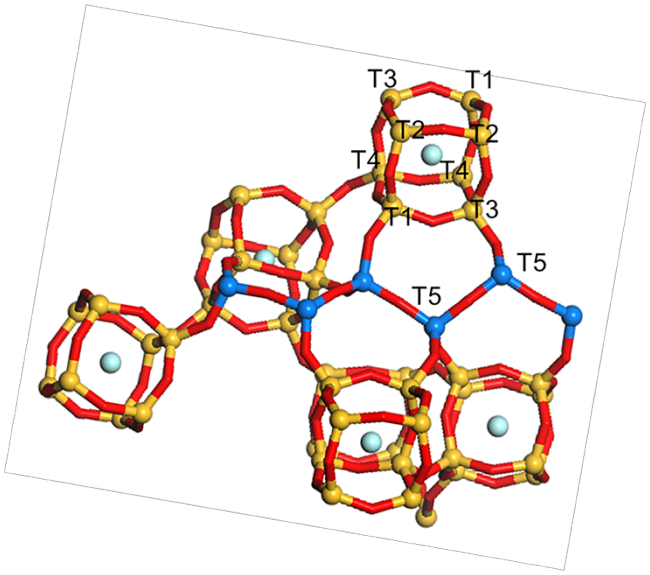

Figure S7. Five crystallographically-independent Si atoms in Si-STW-F: T1–T4 atoms (yellow colored) are involved in the D4R unit, and T5 atoms (blue colored) form chains to connect D4R units in STW-type framework.

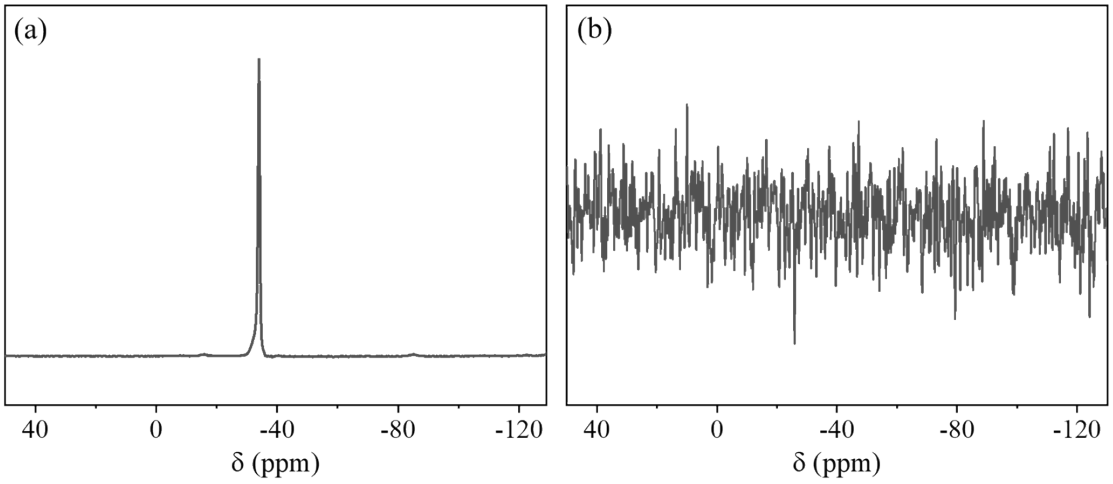

Figure S8. ^{19}F NMR spectrum of (a) Si-STW-F and (b) Si-STW-OH.

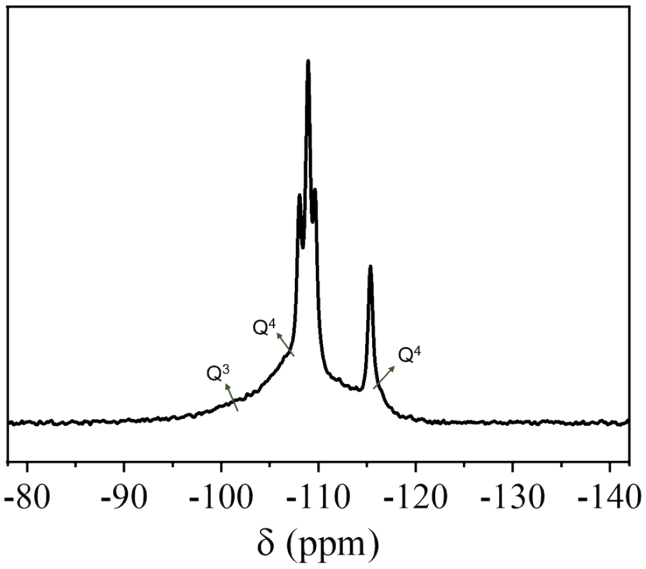

Figure S9. ^{29}Si MAS NMR spectra of Si-STW-OH after calcination.

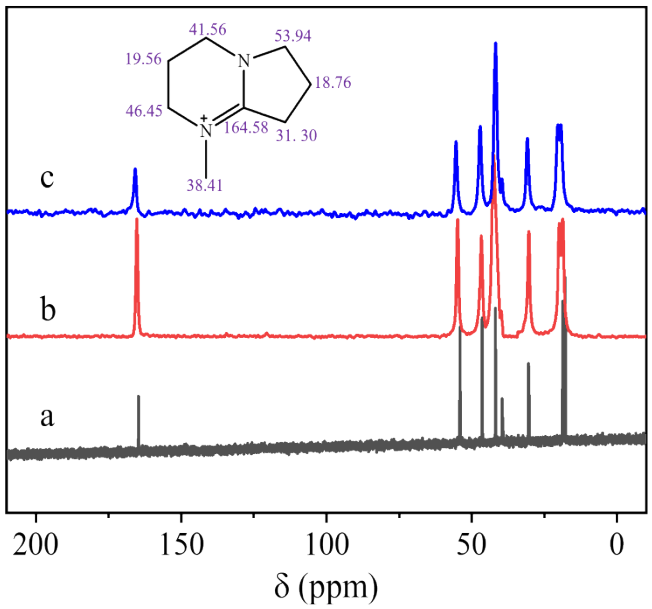

Figure S10. (a) ^{13}C NMR spectra of MDBN in D_2O, and solid state ^{13}C MAS NMR spectra of (b) Si-STW-F and (c) Si-STW-OH.

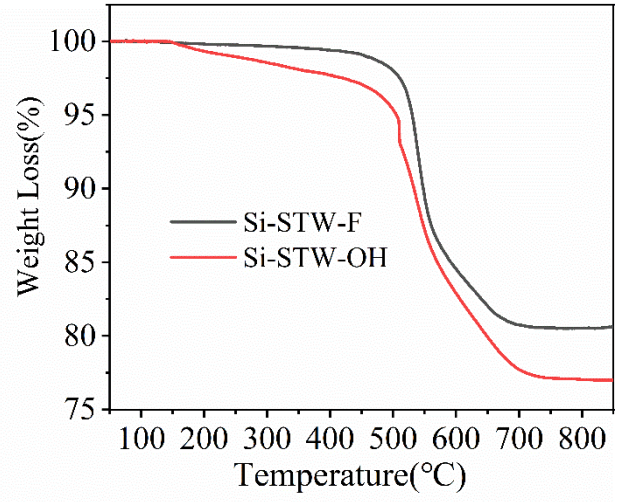

Figure S11. TGA curves of Si-STW-F and Si-STW-OH.

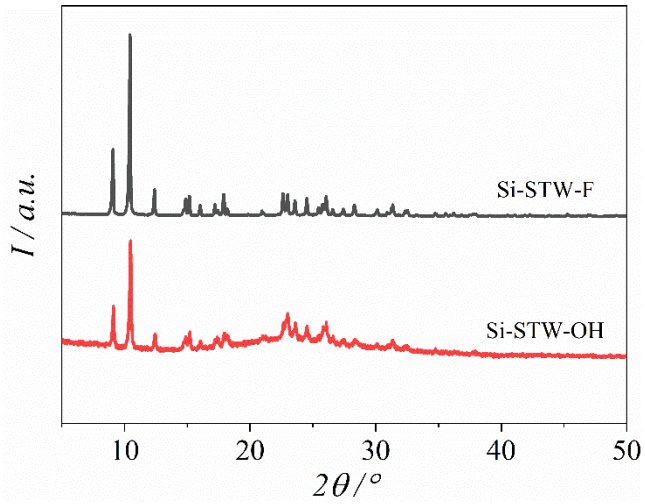

Figure S12. PXRD patterns of calcined Si-STW-F and Si-STW-OH.

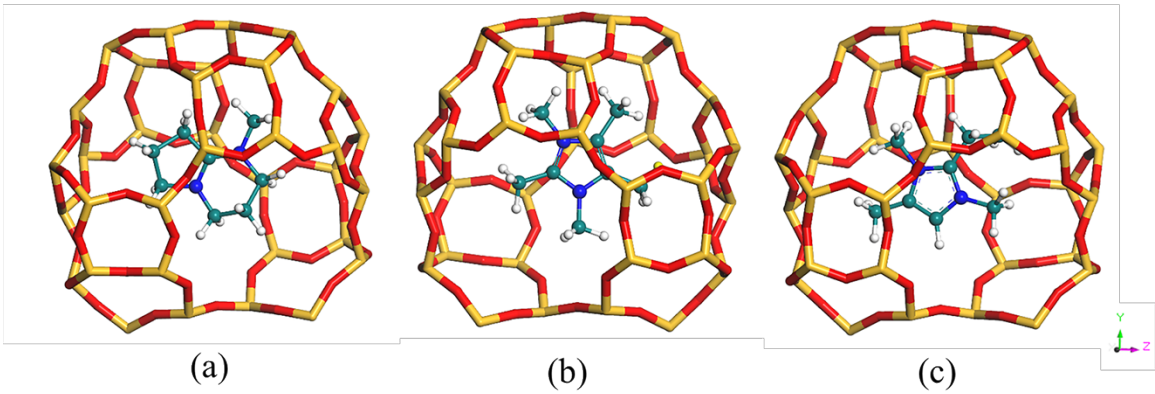

Figure S13. Arrangements of OSDAs in the [$4^6 5^8 8^2 10^2$] cage of Si-STW-F: (a) MBDN, (b) PMI and (c) ETMI,[4] determined by SXRD. Only one possible configuration is shown. Yellow, Si; red, O; cyan, C; white-grey, H; blue, N.

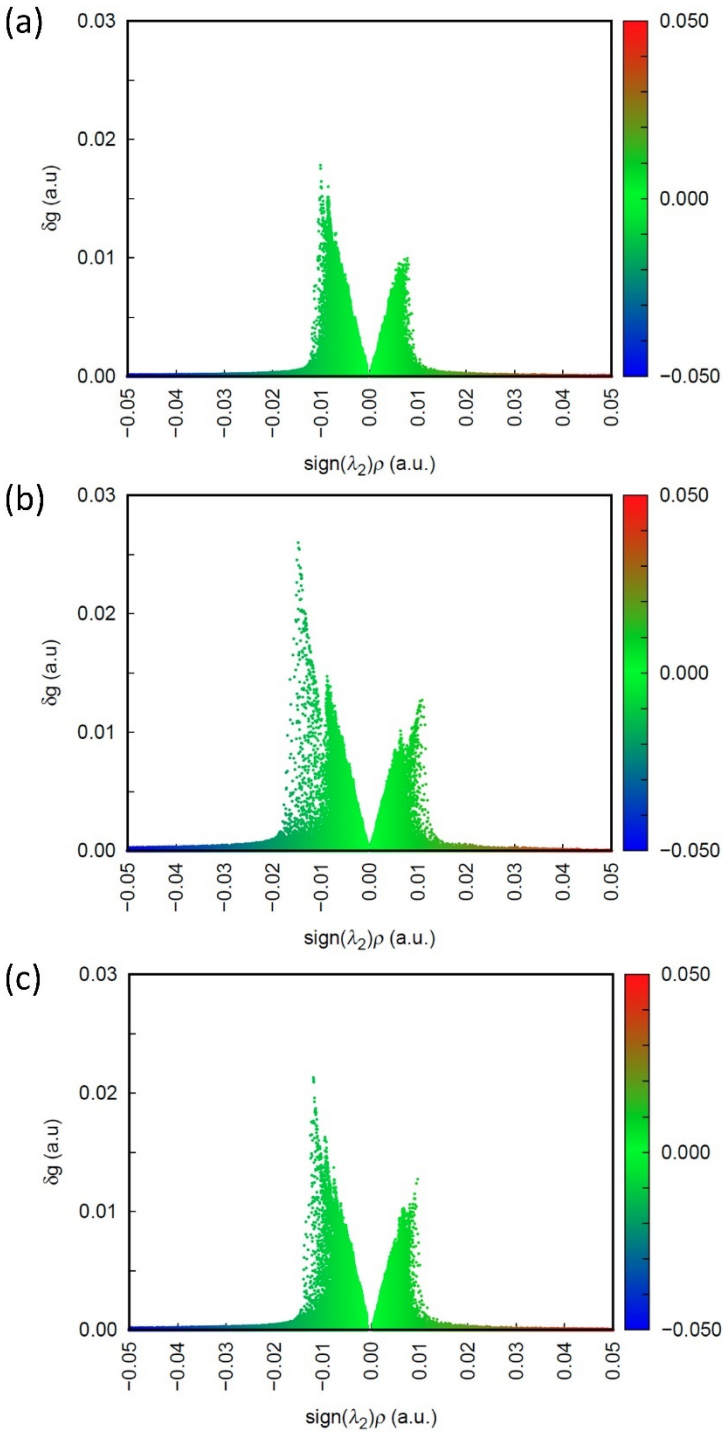

Figure S14. Scatter plots of $\delta_{g\ \mathrm{inter}}$ *vs* sign(λ_2)ρ for (a) MDBN, (b) PMI and (c) ETMI in STW cage, showing intermolecular interactions between the OSDA and the cage. The colour mapping function, sign(λ_2)ρ, indicates whether the interaction is attractive (negative) or repulsive (positive).

Supplementary Tables

Table S1. Synthesis survey for Si-STW-F.

Run	SDA/Si	HF/Si	H_2O/Si	Seed (wt%[a])	Temperature (°C)	Time (d)	Phase[b]
1	1	1	3	0	160	15	STW
2	1	1	5	0	160	15	STW
3	1	1	10	0	160	15	STW
4	0.5	0.5	3	0	160	15	STW
5	0.5	0.5	5	0	160	15	STW
6	0.5	0.5	10	0	160	15	STW
7	0.3	0.3	3	0	160	15	STW
8	0.3	0.3	5	0	160	15	STW
9	0.3	0.3	10	0	160	15	Am + STW
10	0.1	0.1	3	0	160	15	Am
11	0.1	0.1	5	0	160	15	Am
12	0.1	0.1	10	0	160	15	Am
13	0.5	0.3	3	0	160	15	STW
14	0.5	0.3	5	0	160	15	STW
15	0.5	0.3	10	0	160	15	STW
16	0.5	0.1	3	0	160	15	STW
17	0.5	0.1	5	0	160	15	STW
18	0.5	0.1	10	0	160	15	STW
19	0.5	0.5	20	0	160	15	STW
20	0.5	0.5	30	0	160	15	STW
21	0.5	0.5	40	0	160	15	Am + STW
22	0.5	0.5	5	0	160	5	Am
23	0.5	0.5	5	0	160	10	Am + STW
24	0.5	0.5	5	0	160	20	STW
25	0.5	0.5	5	0	160	30	STW
26	0.5	0.5	3	1	160	15	STW
27	0.5	0.5	5	1	160	15	STW
28	0.5	0.5	10	1	160	15	STW

[a] Percentage of theoretical mass of the gel (i.e. the sum mass of SiO_2, OSDAF, and H_2O).

[b] Am: amorphous.

Table S2. Synthesis survey for Si-STW-OH.

Run	SDA/Si	HF/Si	H_2O/Si	Seed (wt%[a])	Temperature (°C)	Time (d)	Phase[b]
29	0.3	0	3	1	160	15	Am
30	0.3	0	5	1	160	15	Am + STW
31	0.3	0	10	1	160	15	Am + STW
32	0.5	0	3	1	160	15	Am + STW
33	0.5	0	5	1	160	15	Am + STW
34	0.5	0	10	1	160	15	Am + STW
35	0.8	0	3	1	160	15	Am
36	0.8	0	5	1	160	15	Am
37	0.8	0	10	1	160	15	Am + STW
38	0.5	0	5	1	160	10	Am
39	0.5	0	5	1	160	20	Am + STW
40	0.5	0	5	1	160	30	STW
41	0.5	0	5	1	160	40	STW
42	0.5	0	5	1	160	50	STW
43	0.5	0	5	0	160	15	Am + STW
44	0.5	0	5	0	160	30	Am + STW
45	0.5	0	5	0	160	50	Am + STW
46	0.5	0	5	1[d]	160	30	Am + STW
47	0.5	0	5	1[d]	160	40	STW
48	0.5	0	5	1[e]	160	40	STW
49	0.5	0	5	1[f]	160	40	STW

[a] All seeds were calcined unless otherwise stated.

[b] Percentage of theoretical mass of gel.

[c] Am: amorphous.

[d] Product from Run 41 pure-silica STW used as seeds.

[e] Product from Run 47 pure-silica STW used as seeds.

[f] Product from Run 41 pure-silica STW used as seeds without calcination.

Table S3. Averaged Si-O-Si angles (°) in as-made Si-STW-F and calcined Si-STW HPM-1.

	T1	T2	T3	T4	T5
As-made Si-STW-F [a]	139.3	140.3	141.3	141.7	155.0
Calcined HPM-1 [b]	146.8	146.4	147.8	148.2	156.3

[a] From single crystal X-ray diffraction analyses.

[b] From Rietveld refinement. [19]

Table S4. Elemental analysis data for Si-STW-F and Si-STW-OH.

samples	C (wt%)	N (wt%)	H (wt%)	C/N [a]	H/N [a]	H/C [a]
Si-STW-F	12.27	3.47	1.94	4.13 (4.0)	7.83 (7.5)	1.90 (1.9)
Si-STW-OH	10.69	3.15	2.12	3.96 (4.0)	9.42 (8.0)	2.38 (2.0)

[a] Molar ratios. Theoretical values of MDBN(F) and MDBN(OH) are given in parentheses.

Table S5. Texture properties of calcined Si-STW-F and Si-STW-OH.

Samples	Si-STW-F	Si-STW-OH
BET surface area, m^2/g	529	496
Micropore surface area, m^2/g	486	440
External surface area, m^2/g	43	56
t-Plot micropore volume, cm^3/g	0.172	0.134
Total pore volume, cm^3/g	0.223	0.201

Table S6. Crystallographic and structural data of Si-STW-F.

Compound reference	Si-STW-F
Empirical formula	$Si_{10}O_{20}(C_8H_{15}N_2F)$
Formula weight	759.12
Temperature/K	210
Crystal system	Hexagonal
Space group	$P6_122$
a/Å	11.8995(9)
b/Å	11.8995(9)
c/Å	29.636(4)
α/°	90
β/°	90
γ/°	120
Unit cell volume/Å^3	3634.2(7)
Z	6
Crystal size/mm^3	0.05 × 0.05 × 0.04
2θ range for data collection/°	3.732 to 53.889
No. of reflections collected	18960
No. of independent reflections	2484
R_{int}	0.0953
R_{sigma}	0.1728
Final R_1 values (I > 2σ(I)) [a]	0.0516
Final wR(F^2) values (I > 2σ(I)) [a]	0.1211
Final R_1 values (all data) [a]	0.0758
Final wR(F^2) values (all data) [a]	0.1305
Goodness of fit on F^2	1.057
CCDC	2211902

[a] $R_1 = \Sigma||F_o| - |F_c||/\Sigma|F_o|$, $wR = [\Sigma w(F_o^2 - F_c^2)^2/\Sigma w(F_o^2)^2]^{1/2}$

Table S7. Atomic coordinates and isotropic thermal parameters of Si-STW-F.

Atom	*x*	*y*	*z*	U(eq)	Occupancy
Si1	-0.0872(2)	0.6625(2)	0.54846(7)	0.0248(5)	1
Si2	0.1159(2)	0.5306(2)	0.63365(7)	0.0260(5)	1
Si3	-0.0955(2)	0.6032(2)	0.64816(7)	0.0257(5)	1
Si4	-0.2989(2)	0.3778(2)	0.53346(7)	0.0261(5)	1
Si5	-0.03011(19)	0.84784(19)	0.69966(6)	0.0207(5)	1
O1	0.0454(5)	0.6714(5)	0.53124(18)	0.0293(13)	1
O2	-0.2139(5)	0.5337(5)	0.53001(18)	0.0329(13)	1
O3	-0.0911(5)	0.6775(5)	0.60221(16)	0.0297(13)	1
O4	0.0291(5)	0.5871(5)	0.65442(17)	0.0328(13)	1
O5	0.1699(7)	0.5849(3)	0.583333	0.0304(18)	1
O6	0.2390(5)	0.5776(5)	0.66711(18)	0.0280(11)	1
O7	-0.2288(5)	0.4671(5)	0.3704(4)	0.0301(13)	1
O8	-0.0970(5)	0.6961(5)	0.68785(16)	0.0262(12)	1
O9	0.1249(5)	0.9137(5)	0.69421(16)	0.0253(12)	1
O10	-0.0690(3)	0.8620(7)	0.75	0.0252(16)	1
O11	-0.0779(6)	0.9221(6)	0.666667	0.0257(16)	1
O12	-0.3571(7)	0.3214(4)	0.583333	0.0317(18)	1
C1	-0.452(3)	0.581(2)	0.6076(10)	0.099(8)	0.5
C2	-0.656(3)	0.359(2)	0.5992(7)	0.089(7)	0.5
C3	-0.738(3)	0.2316(18)	0.6221(7)	0.097(6)	0.5
C4	-0.7758(16)	0.245(2)	0.6692(7)	0.074(5)	0.5
C5	-0.560(5)	0.447(5)	0.6677(11)	0.077(6)	0.5
C6	-0.449(2)	0.530(2)	0.6989(8)	0.097(7)	0.5
C7	-0.479(2)	0.451(3)	0.7420(7)	0.103(7)	0.5
C8	-0.616(2)	0.336(3)	0.7392(6)	0.088(7)	0.5
N1	-0.557(2)	0.458(2)	0.6279(7)	0.086(5)	0.5
N2	-0.6553(15)	0.3351(16)	0.6909(6)	0.080(4)	0.5
F1	-0.0953(8)	0.4524(4)	0.583333	0.055(2)	1

Table S8. Selected interatomic distances (Å) and bond angles (°) of Si-STW-F.

Distances							
Si1-O1	1.611(5)	Si1-O2	1.615(6)	Si1-O3	1.606(5)	Si1-O9	1.620(5)
Si2-O1	1.618(5)	Si2-O4	1.610(6)	Si2-O5	1.625(3)	Si2-O6	1.620(5)
Si3-O3	1.610(5)	Si3-O4	1.597(6)	Si3-O7	1.613(5)	Si3-O8	1.621(5)
Si4-O2	1.612(5)	Si4-O6	1.628(5)	Si4-O7	1.604(5)	Si4-O16	1.628(3)
Si5-O8	1.606(5)	Si5-O9	1.612(5)	Si5-O10	1.596(2)	Si5-O11	1.601(2)
Angles							
O1-Si1-O2	111.9(3)	O1-Si1-O9	105.4(3)	O2-Si1-O9	108.8(3)	O3-Si1-O1	112.8(3)
O3-Si1-O2	112.1(3)	O3-Si1-O9	105.3(3)	O1-Si2-O5	111.3(2)	O1-Si2-O6	103.7(3)
O4-Si2-O1	113.4(3)	O4-Si2-O5	113.2(3)	O4-Si2-O6	106.3(3)	O6-Si2-O5	108.4(3)
O3-Si3-O7	112.8(3)	O3-Si3-O8	104.3(3)	O4-Si3-O3	112.8(3)	O4-Si3-O7	111.9(3)
O4-Si3-O8	109.0(3)	O7-Si3-O8	105.5(3)	O2-Si4-O6	104.4(3)	O2-Si4-O16	115.1(2)
O6-Si4-O16	106.9(3)	O7-Si4-O2	114.0(3)	O7-Si4-O6	104.7(3)	O7-Si4-O16	110.7(2)
O8-Si5-O9	109.2(3)	O10-Si5-O8	108.4(3)	O10-Si5-O9	111.4(2)	O10-Si5-O11	108.12(1)
O11-Si5-O8	112.0(3)	O11-Si5-O9	107.9(3)	Si1-O1-Si2	138.5(3)	Si4-O2-Si1	145.2(4)
Si1-O3-Si3	140.6(3)	Si3-O4-Si2	146.4(4)	Si2-O5-Si2	140.0(5)	Si2-O6-Si4	136.3(3)
Si4-O7-Si3	139.1(4)	Si4-O16-Si4	136.7(5)	Si5-O8-Si3	139.2(3)	Si5-O9-Si1	142.4(3)
Si5-O10-Si5	169.5(5)	Si5-O11-Si5	168.7(5)				

Supplementary References

1 Bruker XPREP (Version 2014/2) and SADABS (Version 2014/4). Bruker AXS Inc., Madison, Wisconsin, USA.
2 L. Krause, R. Herbst-Irmer, G. M. Sheldrick and D. Stalke, *J Appl Crystallogr* 2015, **48**, 3-10.
3 G. M. Sheldrick, *Acta Crystallogr C Struct Chem* 2015, **71**, 3-8.
4 S. J. Clark, M. D. Segall, C. J. Pickard, P. J. Hasnip, M. J. Probert, K. Refson and M. C. Payne, *Z. Krist.* 2005, **220**, 567-570.
5 J. H. Kang, L. B. McCusker, M. W. Deem, C. Baerlocher and M. E. Davis, *Chem. Mater.* 2021, **33**, 1752-1759.
6 J. P. Perdew, K. Burke and M. Ernzerhof, *Phys. Rev. Lett.* 1996, **77**, 3865-3868.
7 S. Grimme, S. Ehrlich and L. Goerigk, *J. Comput. Chem.* 2011, **32**, 1456-1465.
8 S. Grimme, J. Antony, S. Ehrlich and H. Krieg, *J. Chem. Phys*. 2010, **132**, 154104.
9 T. Lu and F. Chen, *J. Comput. Chem.* 2012, **33**, 580-592.
10 J. Zhang and T. Lu, *Phys. Chem. Chem. Phys.* 2021, **23**, 20323-20328.
11 T. Lu and Q. Chen, *J. Comput. Chem.* 2022, ***43***, 539-555.
12 T. D. Kuhne, M. Iannuzzi, M. Del Ben, V. V. Rybkin, P. Seewald, F. Stein, T. Laino, R. Z. Khaliullin, O. Schutt, F. Schiffmann, D. Golze, J. Wilhelm, S. Chulkov, M. H. Bani-Hashemian, V. Weber, U. Borstnik, M. Taillefumier, A. S. Jakobovits, A. Lazzaro, H. Pabst, T. Muller, R. Schade, M. Guidon, S. Andermatt, N. Holmberg, G. K. Schenter, A. Hehn, A. Bussy, F. Belleflamme, G. Tabacchi, A. Gloss, M. Lass, I. Bethune, C. J. Mundy, C. Plessl, M. Watkins, J. VandeVondele, M. Krack and J. Hutter, *J. Chem. Phys.* 2020, **152**, 194103.
13 J. VandeVondele, M. Krack, F. Mohamed, M. Parrinello, T. Chassaing and J. Hutter, *Comput. Phys. Commun.* 2005, **167**, 103-128.
14 C. Hartwigsen, S. Goedecker and J. Hutter, *Phys. Rev. B* 1998, **58**, 3641-3662.
15 S. Goedecker, *Phys. Rev. B* 1996, **54**, 1703-1710.
16 J. VandeVondele and J. Hutter. *J. Chem. Phys*. 2007, **127**, 114105.
17 W. Humphrey, A. Dalke and K. Schulten, *J. Mol. Graphics* 1996, **14**, 33-38.
18 K. Momma and F. Izumi, *J. Appl. Cryst.* 2011, **44**, 1272-1276.
19 A. Rojas and M. A. Camblor, *Angew. Chem. Int. Ed.* 2012, **51**, 3854-3856.

Author Contributions

F. Jiao contributed to the synthesis, analyses and the writing the manuscript.
J. Zhang and Y. Zhao contributed to the structure solution.
X. S. Cai, H. Li, and Y. N. Xu contributed to the data analysis.
H. B. Du administrated the work, carried out theoretical calculations, and wrote the manuscript.